Influence of temperature on the performance of an evaporation driven micro pump

µFLU14-18

INFLUENCE OF TEMPERATURE ON THE PERFORMANCE OF AN EVAPORATION DRIVEN MICRO PUMP

Chuan Nie[1], Arjan Frijns[1], Rajesh Mandamparambil[2] and Jaap den Toonder*[1]
[1]Eindhoven University of Technology, Post Box 513, 5600MB Eindhoven, the Netherlands
c.nie@tue.nl, a.j.h.frijns@tue.nl, j.m.j.d.toonder@tue.nl
[2]Holst Centre, Post Box 8550, 5605 KN Eindhoven, the Netherlands
rajesh.mandamparambil@tno.nl

KEY WORDS

Flexible system, Microfluidics, Laser fabrication, Foil technology.

ABSTRACT

Microfluidic devices are important for health care applications. Some of the applications require a continuous liquid flow over a sensor surface, which can be accomplished by an evaporation driven pump.

We have realized an evaporation driven pump on a multilayer substrate foil fabricated by lasers. The structures are ablated on polyethylene terephthalate (PET) stacked foils with an inlet and an outlet, and connected by a microchannel. At the outlet, the liquid evaporates via a porous structure. The capillarity of the channel surface keeps the meniscus in the pores and pushes the liquid towards it thereby generating a flow in the channel with a magnitude that is determined by the evaporation rate. The temperatures of the liquid and the ambient determine the vapor concentration difference and thereby influence the evaporation rate. The goal of this paper is to investigate the effects of temperature on the flow rate in the evaporative micro pump in order to achieve appropriate and controllable flow rates.

In our experiments, the flow in the channel is measured using 2D-particle tracking velocimetry. The results are compared with values estimated from an evaporation theory that includes a correction factor for the geometry of the porous structure, since the distribution of pores influences the evaporation. By heating the device creating a temperature difference of 9.4 °C between the substrate and the ambient, the flow rate is increased by 130% compared to the unheated case . These experimental values are in a good agreement with predictions by the evaporation model.

1. INTRODUCTION

Microfluidic devices are important for health care applications, especially for lab-on-chip devices and body liquid sensing such as sweat monitoring. Often, these applications require a continuous liquid flow over a sensor surface. Various micro pumping mechanisms have been studied for small scale devices.[1–4] Here we focus on an evaporation driven micropump. Evaporation, as a natural phenomenon, can be utilized as a driving force for pumping. The control of the evaporation rate plays a key role in reaching appropriate and controllable flow rates. The evaporation of water in air is sensitive to the temperature of both water and air. The goal of this paper is to investigate the effects of temperature on the flow rates in such an evaporative micro pump.

In this paper, we present an evaporation driven pump which is structured on a flexible foil substrate. It is compatible with volume production such as roll-to-roll manufacturing.[5] Water is used as the model liquid in the system. The device is evaluated by measuring the flow rate. The flow rate of the pump is controlled by varying geometrical parameters of its outlet and the temperature of the liquid. The effects of other ambient parameters such as room temperature and humidity will be discussed as well. The results will be evaluated using a theoretical evaporation model that is discussed in the next section.

* Corresponding author

2. EVAPORATION MODEL

Our microfluidic pump has a single inlet. The outlet is covered with an array of small micro-pores (Fig. 1). Liquid is transported from the inlet to the outlet via a capillary channel. The flow in the channel is generated totally by evaporation, governed by volumetric equilibrium:

$$Q = -\frac{dm}{\rho dt}, \tag{1}$$

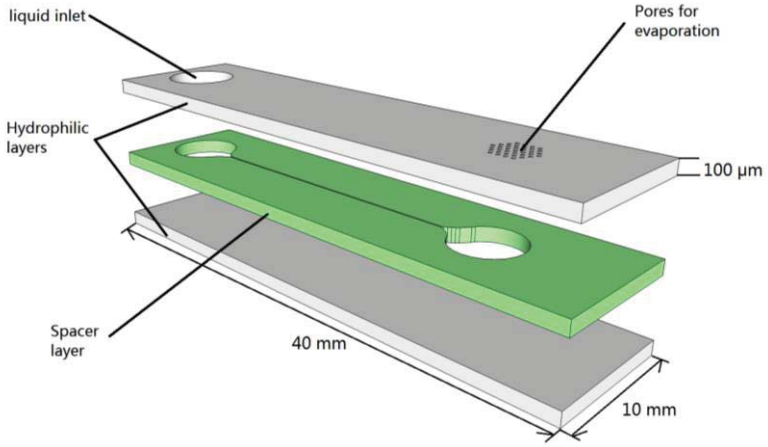

Figure 1 The structure of test sample, layer materials: white, hydrophilized polyethylene terephthalate (PET); green, PET with adhesive coated on both sides.

where Q is the volumetric flow rate in the channel, $-\frac{dm}{dt}$ is the mass loss rate by evaporation, and ρ is the density of the liquid in the system.

First we consider the evaporation from a single sessile droplet, which we assume to model the evaporation from a single pore. The evaporation rate (mass loss rate) can be estimated by: [6]

$$\left(\frac{dm}{dt}\right)_{SINGLE} = -2\pi DM[c(T_w) - Hc(T_a)]F(\theta)a, \tag{2}$$

where D is diffusivity of the liquid molecules, M is the molar mass of the liquid, $c(T_w)$ and $c(T_a)$ are the vapor concentrations at water temperature T_w and ambient temperature T_a, H is the relative humidity, $F(\theta)$ is a function of contact angle θ, and a is the contact radius of the droplet. In our case, we approximate the meniscus of the drop in a single pore by a flat surface, and in that case $F(\theta) = 2/\pi$.[7,8]

Considering the fact that the outlet is a porous structure consisting of multiple pores, the evaporation rate is not simply given by multiplying the mass loss rate as found in Eq. (2) by the number of pores, because the evaporation of a droplet in an array (DIA) is influenced by its neighbors. Due to this interaction, the evaporation rate per pore is reduced compared to the single droplet / pore case. The evaporation correction factor (ECF) [7,8] $\eta_{DIA}, (\eta_{DIA} \le 1)$ is therefore introduced as:

$$\left(\frac{dm}{dt}\right)_{DIA} = \eta_{DIA}\left(\frac{dm}{dt}\right)_{SINGLE}, \tag{3}$$

In an array of N droplets, the ECF of the i-th droplet (η_i) located at position r_i follows: [9]

$$\eta_i + \sum_{j=1, j\neq i}^{N}\left(\eta_i \frac{a_i}{|r_i - r_j|}\right) = 1 . \tag{4}$$

In our case, the total evaporation rate can be estimated as:

$$\left(\frac{dm}{dt}\right)_{TOTAL} = \sum_{i=1}^{N}\left[\eta_i\left(\frac{dm}{dt}\right)_{SINGLE}\right] . \tag{5}$$

If the pores are arranged in an array structure whose pores have same diameter and $F(\theta)$, and $\left(\frac{dm}{dt}\right)_{SINGLE}$ is the same for each pore, Eq. (5) can be simplified to:

$$\frac{dm}{dt} = N\bar{\eta}\left(\frac{dm}{dt}\right)_{SINGLE}, \tag{6}$$

where the mean ECF is

$$\bar{\eta} = N^{-1}\sum_{i=1}^{N}\eta_i \,. \tag{7}$$

The total evaporation rate is then as follows:

$$\frac{dm}{dt} \propto \bar{\eta} Na \quad . \tag{8}$$

According to the calculation of ECF, a normalized evaporation rate figure can be drawn as a function of the number of pores, as shown in Fig. 2.

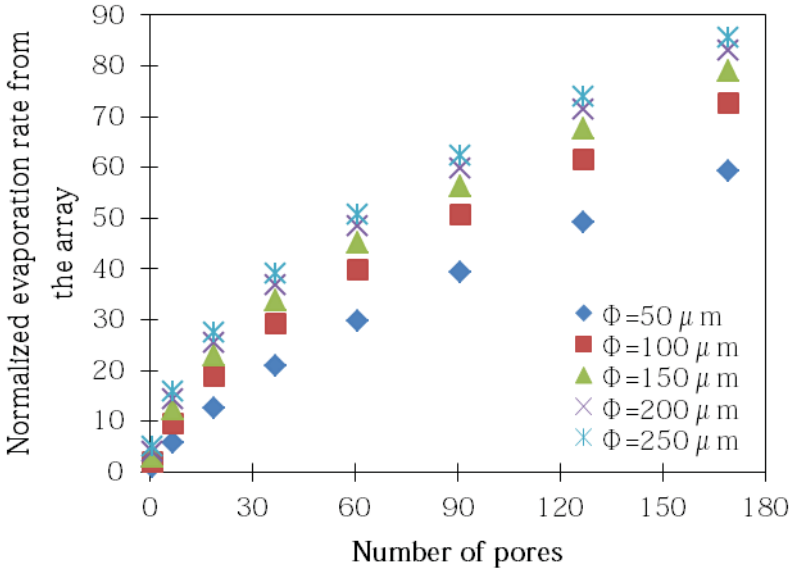

Figure 2 Normalized evaporation rate through a regular array of pores, as a function of the number of pores. Normalized with respect to a single pore with 50 µm diameter (Φ).

In Fig.2, the calculated evaporation rate in the whole array is increased by both increasing the size and the number of pores. The increase is non-linear with respect to either the diameter or the number of the pore array due to the evaporation correction factor. Theoretically, the increase of the total evaporation rate is slowing down for a high diameter porous structure or for large number of pores.

3. EXPERIMENTS

3.1 Design and Fabrication

The total design of our test sample is shown in Fig. 1. The sample is made of three layers of polyethylene terephthalate (PET) based materials. The top and bottom layers single side hydrophilized PET and the middle layer is a spacer layer with an adhesive at both sides of a PET backbone. Each PET layer has a thickness of around $100\mu m$, and the dimensions of the sample is approximately $40mm \times 10mm \times 300\mu m$. The structures, except for the pores at the outlet, are fabricated by a CO_2 laser cutter. A straight microchannel connects the inlet and outlet and is structured in the middle spacer layer. At the outlet, the top part is covered with a porous structure. The pores in the structure is distributed hexagonally, with a fixed pitch of $500\mu m$. The porous structure $(diameter = 250\mu m, pitch = 500\mu m)$ in the top layer is ablated by a excimer laser. The microchannel in the spacer layer has a width of $178\mu m$. The whole sample is laminated using a rubber roller.

3.2 Flow experiments

After fabrication of the sample, water with tracer particles (R0200B, Thermo Scientific particle diameter $= 2\mu m$) is prepared for flow experiments. The experimental setup is shown schematically in Fig. 3. When a droplet of water is put at the inlet, the whole system is filled by capillarity. Then the liquid evaporates via the pores at the outlet, hence generating a flow in the channel. For measuring the flow rate in the channel, a setup of two-dimensional particle tracking velocimetry (2DPTV) is used. The movements of the tracer particles are recorded by a digital camera (Altra 20) mounted on a microscope (Olympus BX51). A heater controlled by a voltage source is used to control the temperature of the sample to enhance the evaporation, in order to achieve a higher flow rate. The temperature rise of the surface is recorded by a thermocouple which is attached onto the surface of the heater. Environmental conditions such as temperature and humidity are measured by a separate sensor (IST HYT-271).

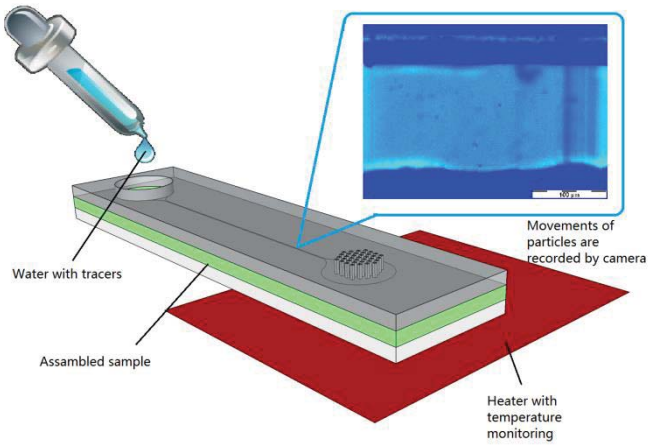

Figure 3 Experimental setup: Heat enhanced evaporation driven flow experiment.

The movements of tracers in the microchannel are recorded as video files. Every recording lasts one minute and multiple files are documented for each temperature setting. Using the measured velocity profiles, the volume rate in the microchannel can be determined.

4. RESULTS AND DISCUSSIONS

The flow rates measured in our experiments are presented in Fig. 4. The theoretical values are calculated by Eqs. (6) and (7)with input of the monitored environmental conditions during the experiments.

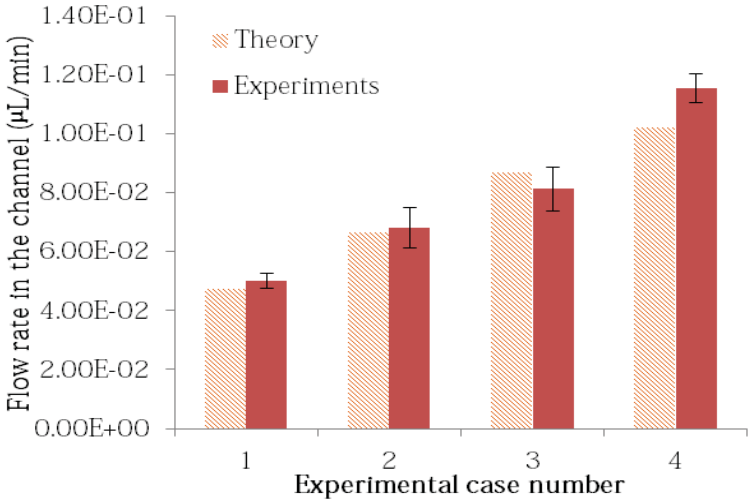

Figure 4 Experimental data of evaporation driven flow experiments (37 pores): conditions for case 1-4: 1, no heating,: room temperature; 2,3 and 4, substrate is heated 4, 7.2, and 9.6 °C above room temperature, respectively.

A good agreement between the theoretical and experimental values is found. The differences can be ascribed to several aspects such as the measurement accuracy of temperature and humidity, geometrical differences between droplets and the actual meniscus in the pores and the measurement precision of the

2DPTV experiments. Since the vapor concentration $c(T)$ is quite sensitive to temperate T, a variation of environmental temperature by only 1°C can give a deviation of 5% in evaporation rate. Also, in our experiments, the liquid meniscus is located at the bottom of the pores, i.e. it is present in well structures formed by the pores in the top PET layer, and therefore the evaporation rate may be reduced compared to the sessile droplet case. In addition the flow profile measured by 2DPTV may be underestimated due to a deviation of the focal plane of the microscope from the mid plane of the rectangular channel which would cause an underestimation of the measured total flow rate. Finally, the experiments are done in a box to avoid air flow over the sample, but it is not a totally closed system and cannot completely prevent the flow in the box due to the temperature gradient caused by devices such as the camera and the light source. A flow over the liquid-gas interface would enhance the evaporation and would give errors as well.

5. CONCLUSIONS

We manufactured a micropump on a foil that is driven by evaporation. The experimentally determined flow rates show good agreement with the evaporation rate calculated by an evaporation theory that includes an evaporation correction factor. By controlled heating of the evaporation structure of the micropump, a clear enhancement of evaporation and therefore a higher flow rate are obtained. The enhancement is predictable from the evaporation theory if the environmental parameters such as temperature and humidity are known.

ACKNOWLEDGEMENTS

This work is supported by NanoNextNL (sub-project 10A), a micro and nanotechnology program of the Dutch government and 130 partners. This project is carried out in collaboration with Holst Centre, Eindhoven, the Netherlands.

REFERENCES

[1]Van Lintel, H. T. G., van De Pol, F. C. M., & Bouwstra, S. (1988) A Piezoelectric Micropump Based on Micromachining of Silicon. *Sens. Actuators*, **15**, 153–167.

[2]Lemoff, A. V., & Lee, A. P. (2000) An AC Magnetohydrodynamic Micropump. *Sens. Actuators B Chem.*, **63**, 178–185.

[3]Yun, K.-S., Cho, I.-J., Bu, J.-U., Kim, C.-J., & Yoon, E. (2002) A Surface-Tension Driven Micropump for Low-Voltage and Low-Power Operations. *J. Microelectromechanical Syst.*, **11**, 454–461.

[4]Zimmermann, M., Schmid, H., Hunziker, P., & Delamarche, E. (2007) Capillary Pumps for Autonomous Capillary Systems. *Lab. Chip*, **7**, 119–125.

[5]Van den Brand, J., de Baets, J., van Mol, T., & Dietzel, A. (2008) Systems-in-Foil – Devices, Fabrication Processes and Reliability Issues. *Microelectron. Reliab.*, **48**, 1123–1128.

[6]Semenov, S., Starov, V. M., Velarde, M. G., & Rubio, R. G. (2011) Droplets Evaporation: Problems and Solutions. *Eur. Phys. J. Spec. Top.* **197**, 265–278.

[7]Picknett, R., & Bexon, R. (1977) The Evaporation of Sessile or Pendant Drops in Still Air. *J. Colloid Interface Sci.*, **61**, 336–350.

[8]Schönfeld, F., Graf, K.-H., Hardt, S., & Butt, H.-J. (2008) Evaporation Dynamics of Sessile Liquid Drops in Still Air with Constant Contact Radius. *Int. J. Heat Mass Transf.*, **51**, 3696–3699.

[9]Kokalj, T., Cho, H., Jenko, M., & Lee, L. P. (2010) Biologically Inspired Porous Cooling Membrane Using Arrayed-Droplets Evaporation. *Appl. Phys. Lett.*, **96**, 163703–163703–3.